Boiling Heat Transfer in Rectangular Channels of Small Gaps

Yang, Yang
Department of Mechanical Engineering Science : Graduate Student

Fujita, Yasunobu
Department of Mechanical Engineering Science : Professor

出版情報：九州大学工学紀要. 62 (4), pp.223-239, 2002-12-20. 九州大学大学院工学研究院
バージョン：
権利関係：

Memoirs of the Faculty of Engineering, Kyushu University, Vol. 62, No. 4, December 2002

Boiling Heat Transfer in Rectangular Channels of Small Gaps

by

Yang YANG* and Yasunobu FUJITA**

(Received September 25, 2002)

Abstract

An experimental investigation was conducted to elucidate boiling heat transfer and flow pattern in a narrow-flat rectangular channel of a 100 mm-heated length with R-113 as the test fluid. The cross section of the channel is 20 mm wide and its height (referred to the gap) is varied as 0.2, 0.5, 1.0 and 2.0 mm to form a narrow boiling space. It was found that heat transfer coefficient is a complex function of mass velocity, heat flux and vapor quality for a given value of the gap size. In the downstream of the onset point of nucleation there follows the bubbly flow region of nucleate boiling dominance. This region is localized rather shortly in the present narrow channels and replaced by the regions of successive slug and annular flows where convective evaporation becomes dominant. Heat transfer coefficient in the slug and the annular flow regions increases in the flow direction under some thermal and hydrodynamic conditions until dry-out quality is approached, while for another conditions heat transfer coefficient decreases steadily in the flow direction. This steady decrease is observed when the gap size is small, mass velocity low and heat flux is high. In the present narrow channels five flow patterns are identified: (a) bubbly flow of spherical bubbles, (b) bubbly flow of two-dimensionally flattened bubbles, (c) coexistence of slug and bubbly flows, (d) slug flow, and (e) annular flow. A smaller gap of the narrow channels gives higher heat transfer coefficients when heat fluxes are low, whereas heat transfer deterioration begins at lower quality as heat flux becomes higher.

Keywords: Mini-channel, Narrow rectangular channel, Flow boiling, Flow pattern, Influence of channel gap

*Graduate Student, Department of Mechanical Engineering Science
**Professor, Department of Mechanical Engineering Science

1. Introduction

Microscale heat transfer is currently of great interest due to highly efficient means for heat exchange and finds many potential applications in a wide variety of advanced technologies. Previous investigations on transport process in microscale systems have shown that microscale transport process has distinctively different thermal and hydrodynamic properties as compared to those for conventional systems. As well as microscale heat transfer, miniscale heat transfer is also paid much attention because it shows several preferable characteristics and it builds a bridge between heat transfer of conventional size and micro-size systems.

It is known from the past investigations that in very small or narrowly confined space or channels where hydraulic diameter is of the same order or less than the bubble size, boiling heat transfer and flow behavior are substantially different from those encountered in flow channels of conventional size. Heat transfer is enhanced in some cases, while significantly deteriorated in another cases. Thus in designing micro- or mini-cooling devices, it is prerequisite to know heat transfer characteristics and plausible mechanisms of heat transfer enhancement and deterioration. Because of the complexity of boiling phenomena and the lack in enough research works in this field, however, boiling heat transfer in small- or mini-channels is still far from well understood.

Peng and Wang[1] performed experiments in rectangular-shaped micro-grooves machined into stainless steel plates with methanol as the test fluid. They noted that liquid velocity, subcooling, fluid properties and the micro-channel geometry have significant influences on heat transfer characteristics, cooling performance and flow pattern transition. In their experiment, however, fluid velocity and subcooling appear to have no obvious effect on heat transfer in the fully developed nucleate boiling region, although they may significantly alter the onset point of nucleate boiling.

Bao et al.[2] and Lin et al.[3] performed experiments of two-phase flow and heat transfer in small horizontal tubes of 1.95 mm and 1 mm diameter, respectively. Bao et al.[2] indicated that heat transfer coefficient is a strong function of heat flux and system pressure, while the influence of mass velocity is insignificant.

One of the present authors[4] measured boiling curves for a vertical flat channel set in water pool and found that boiling heat transfer is enhanced in comparison with pool boiling in a wider space until heat flux reaches a certain level. For higher heat fluxes exceeding this level, boiling heat transfer is rapidly deteriorated and critical heat flux is attained at rather low level compared to critical heat flux in pool boiling.

Yu et al.[5] experimentally investigated pressure drop and heat transfer to water in a small horizontal tube of a diameter of 2.98 mm and a heated length of 910 mm. Measured boiling heat transfer coefficients are dependent on heat flux while independent of mass velocity. This behavior means that nucleate boiling dominates over convective evaporation, and the nucleate boiling dominance persisted to vapor quality exceeding 0.5.

Tran et al.[6] experimented boiling heat transfer in a small tube of 2.46 mm diameter and a small rectangular channel (hydraulic diameter $d_h=2.40$ mm) with refrigerant R-12 as the test fluid. At all wall superheats except the lowest value in their experiments, heat transfer was found dependent on heat flux but independent of mass velocity in the quality range from 0.2-0.8. In the low wall superheat region of $\Delta T_{sat}<2.75$°C, forced convection mechanism dominated. The circular-tube and the rectangular-channel showed very little difference in heat transfer coefficients when compared for the same values of hydraulic diameter.

Triplett et al.[7] investigated flow patterns and void fraction of gas-liquid two-phase flow in long horizontal small-channels of the circular and semi-triangular cross-sections. Hydraulic diameters of the test sections were 1.1 and 1.45 mm for the circular tube and 1.09 and 1.49 mm for the semi-triangular channel. They distinguished five major flow patterns: bubbly, slug, churn, slug-annular, and annular flow.

The object of the present study is to experimentally investigate heat transfer and flow pattern for flow boiling in narrow channels and to make sure their difference and/or similarity to flow boiling in conventional size of channels. For visual observation a flat channel of rectangular cross-section of small gaps is used as the test section in the present experiment. The one side is the heated surface and the opposite side is the glass plate through which boiling phenomena are visualized. Experimental variables are mass velocity, heat flux, vapor quality and the gap size of channel.

2. Experimental Apparatus

A schematic diagram of experimental flow loop is shown in **Fig. 1**. It consists of a reservoir, liquid circulation pump, flow meters, preheater, test section, condenser, and flow control valves. Test fluid is pumped from the reservoir, flowing through one of two flow

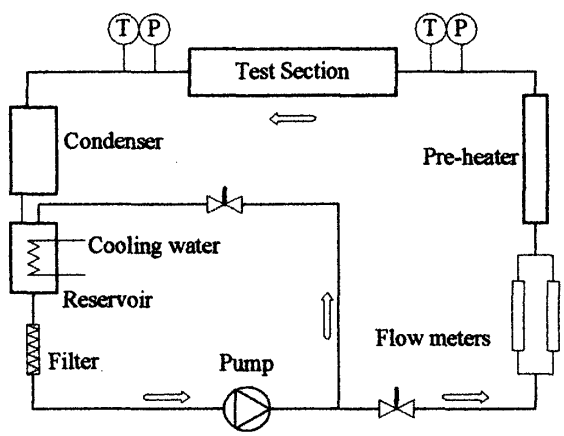

Fig. 1 Experimental flow loop

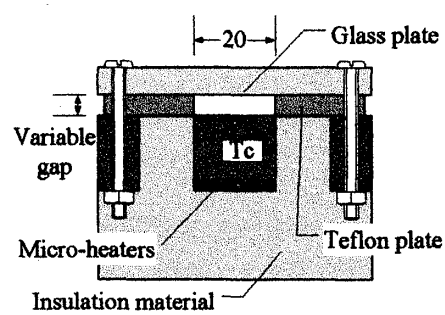

Fig. 2(a) Test section

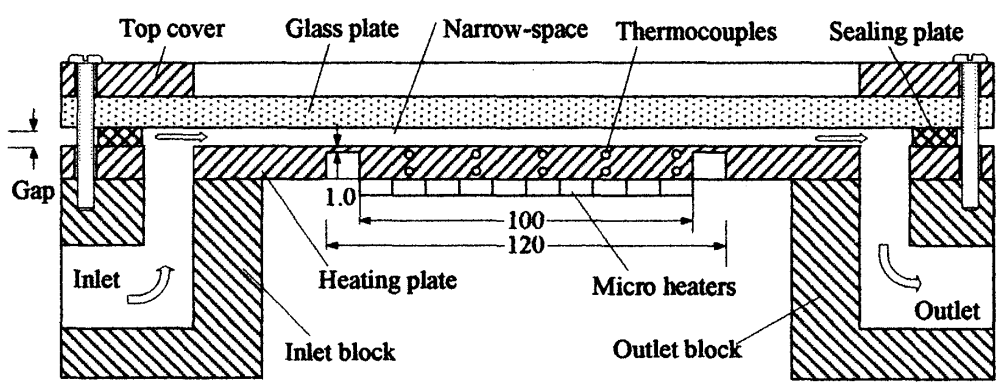

Fig. 2(b) Test section

Table 1 Experimental Range

Test section inlet pressure	106~118 kPa, 102~170kPa (H=0.2mm)
Mass velocity	100, 200, 500 kg/m^{2}s
Heat flux	2000~90000 W/m^2
Gape size	0.2, 0.5, 1, 2 mm

meters and the preheater, and enters the test section. A bypass loop is used to control the flow rate sent to the test section by circulating an excess amount of the pumped fluid directly to the reservoir. Fluid subcooled temperature or vapor quality at the inlet of the test section is adjusted by changing power input to the preheater.

Figure 2(a) shows a cross-sectional view of the test section that has a rectangular cross section with the height H (referred to the gap size hereafter) much smaller than the width W. The rectangular heating section is $W=20$ mm wide and $L=100$ mm long, while the gap size is changed as $H=0.2$, 0.5, 1.0 and 2.0 mm. The lower plate of the horizontal test section is made of copper and serves as the heating surface. The upper unheated plate is made of Pyrex glass through which flow visualization is done. The side thin plates are made of Teflon. This Teflon side plates of specified thickness set up the narrow channels.

Figure 2(b) shows another sectional view seeing from the side. The unheated calming sections of 29 mm long are provided at the upstream and downstream of the heated test section respectively. Thus, 158 mm is the total length of the test section, which is smoothly connected to the mixing chambers.

Heat flux to the test fluid from the heating surface is supplied by ten micro-heaters, 10 mm times 20 mm each, pressed to the bottom surface of the heating copper plate. Heating surface temperature are measured at five locations in the flow direction that are at the distance of 10, 30, 50, 70 and 90 mm from the starting point of the heated section and at the center of the channel width. In each location two pair of thermocouples are imbedded in the copper plate at the depths of 1.2 and 8.8 mm under the surface. The heating surface temperature and heat flux at each locations are determined from the measured temperatures assuming one-dimensional heat conduction. Fluid temperature and pressure at the inlet and outlet of the test section are measured in the mixing chambers.

The experiments are conducted with refrigerant R-113 as the test fluid (the saturation temperature is 47.59°C for 0.1013 MPa). Main variable parameters in the present experiment are mass velocity, heat flux, vapor quality and the gap size of the channel. Their ranges and other relevant parameters are indicated in **Table 1**.

3. Results and Discussion

3.1 Flow Patterns and Regimes

Boiling flow patterns were visually observed through the upper Pyrex glass plate over the whole length of the test section. Flow structures were photographed by using a color CCD camera and a high-speed video camera.

Figure 3 shows typical pictures of various flow patterns observed in the channel of the gap size of $H=0.5$ mm, the left column for $G=200$ kg/m^{2}s and the right column for $G=100$ kg/m^{2}s. The flow direction is from the left to right, and the field of picture is 45 mm times 20 mm. Pictures are arrayed in the increasing order of vapor quality from the top to bottom. The center of picture corresponds to the center of heating surface in the flow direction. Values of vapor quality, wall superheat and heat transfer coefficient are given under each picture for reference. These values are evaluated at $z=50$ mm. All of these pictures were taken at a nearly same heat flux of $q=20$ kW/m^2 by maintaining power input to the test section heaters at constant and increasing power input to the preheater from zero to high value step by step.

As seen in these pictures, flow structures characterized by the size and shape of each vapor bubble or vapor slug, the number of vapor bubbles or slugs, the liquid-vapor interface

H=0.5mm, G=200 kg/m^{2}s

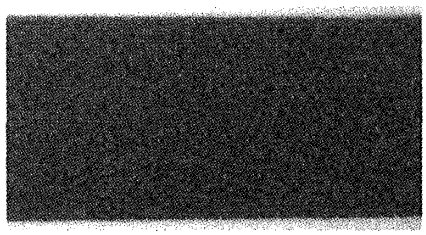

Spherical bubble flow

x=0.01, ΔT=5.7K, α=3.7kW/m^2 K

Flattened bubble flow

x=0.03, ΔT=4.9K, α=3.7kW/m^2 K

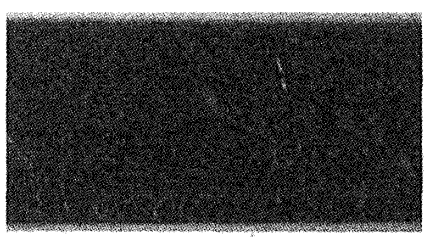

Slug and bubble flow

x=0.06, ΔT=5.6K, α=4.1kW/m^2 K

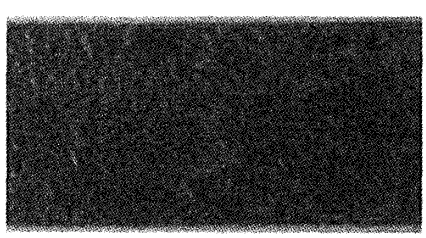

Slug flow

x=0.16, ΔT=13.4K, α=3.8kW/m^2 K

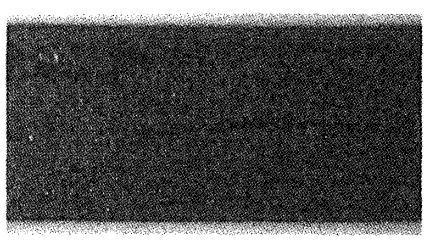

Annual flow

x=0.30, ΔT=22.3K, α=3.8kW/m^2 K

H=0.5mm, G=100 kg/m^{2}s

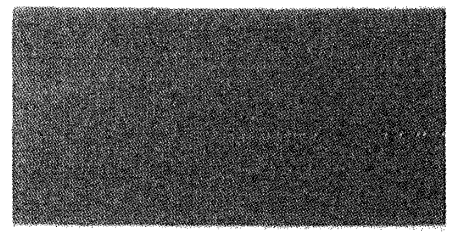

Spherical bubble flow

x=0.00, ΔT=3.7K, α=1.6kW/m^2 K

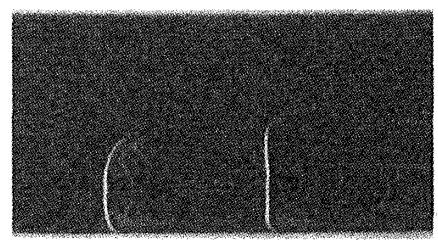

Flattened bubble flow

x=0.01, ΔT=3.8K, α=3.3kW/m^2 K

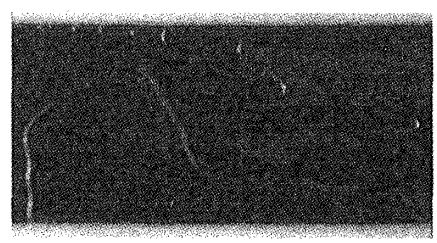

Slug and bubble flow

x=0.04, ΔT=3.9K, α=3.9kW/m^2 K

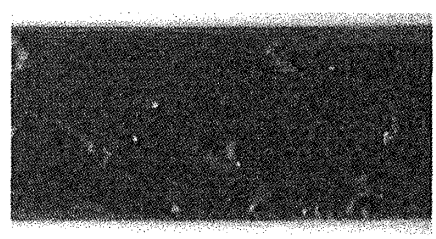

Slug flow

x=0.15, ΔT=9.2K, α=3.6kW/m^2 K

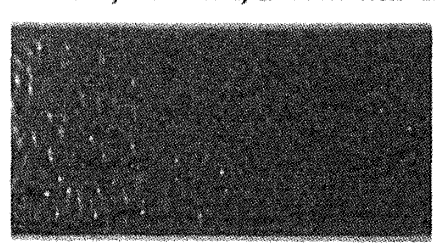

Annual flow

x=0.34, ΔT=20.31K, α=2.9kW/m^2 K

Fig. 3 Flow patterns of $H=0.5$ mm

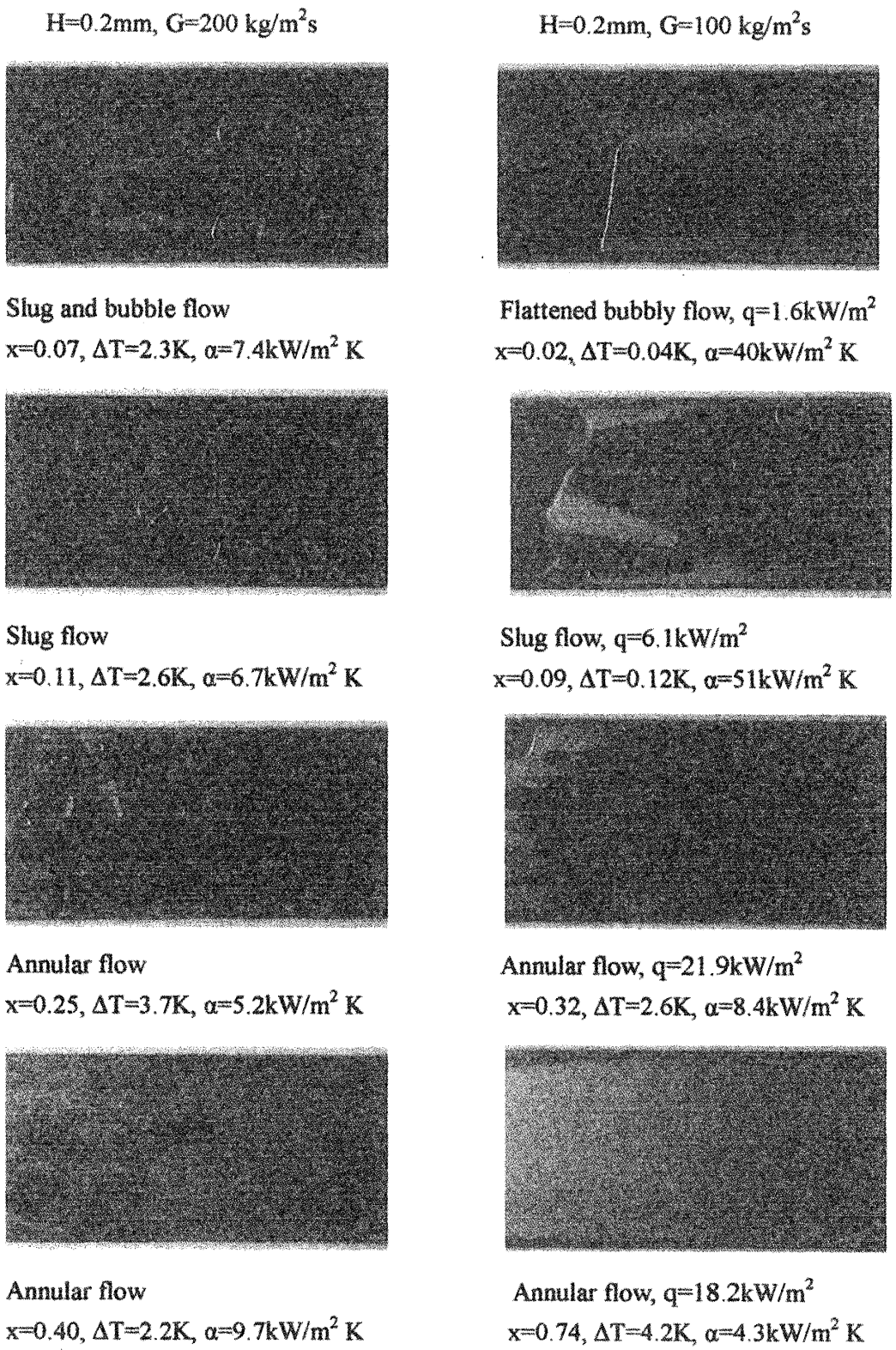

Fig. 4 Flow patterns of $H = 0.2$ mm

patterns are definitely different between the pictures. From a close examination of the whole still and video pictures taken in the present experiment, it is found that flow patterns observed in the present narrow channels are classified in the following typical five types: (a) bubbly flow of spherical bubble shape in the subcooled or low-quality boiling region, as seen in pictures on the first row in **Fig. 3**, where bubbles are less than the gap size, growing in an

isolated spherical form and sliding in the downstream direction until the bubble reaches the upper wall at a some downstream location. (b) Bubbly flow of two-dimensional circular shape of bubble in the saturated nucleate boiling region (2nd row in **Fig. 3**). The bubble growth rate is increased as heat flux or heating wall superheat is increased in the saturated region. Thus, the bubble top rapidly reaches the upper channel wall, and thereafter bubbles are forced to grow in the lateral direction, thus bubbles are flattened and take a form of sliced two-dimensional oblate circle. (c) Slug and bubbly flow where several oblate bubbles merge to form large vapor slugs, while other bubbles remain as isolated oblate bubbles (3rd row in **Fig. 3**). Once a vapor slug is formed in the channel, it grows fast to absorb surrounding isolated bubbles and extends to the whole channel width. (d) Slug flow where a large vapor slug occupies the channel width and its growth is in the longitudinal direction (4th row in **Fig. 3**). Tiny isolated bubbles are still remaining in the area between neighboring slugs. (e) Annular flow where elongated slugs merge to cover all the channel space and vapor flows as a continuous phase (5th row in **Fig. 3**). Most liquid takes a form of thin film on the peripheral wall of the channel. These five patterns identified in the present experiment of boiling two-phase flow are basically similar to those observed by Xu[8] for adiabatic air-water two-phase flow in vertical rectangular channels of the gap size of 1.0 and 0.6 mm.

Figure 4 shows several typical pictures of flow patterns observed for the smallest gap size of $H=0.2$ mm in the present experiment. The left column indicates the pictures of $G=200$ kg/m^{2}s, which are taken at a nearly same heat flux of $q=20$ kW/m^2. The right column shows the pictures for $G=100$ kg/m^{2}s but for different heat fluxes ranging 1.6 to 22 kW/m^2. For mass velocity of $G=100$ kg/m^{2}s, vapor quality increases too fast to catch all flow patterns. Comparing pictures for $H=0.5$mm in **Fig. 3** and pictures for $H=0.2$ mm in **Fig. 4**, we can find some similarity and difference between flow patterns. First of all, the spherical bubble flow does not exist at $H=0.2$ mm. Even the uppermost picture of $G=100$ kg/m^{2}s on the right column in **Fig. 4** may be classified to flattened bubbly flow, but it looks like rather a kind of slug flow. This means that all bubbles merge to form a big single slug just at the time they generate. In the whole experiments for $H=0.2$ mm, small isolated bubbles never exists, at least stable isolated bubbles are not observed. The third and the fourth rows in **Fig. 4** both indicate annular flow, but the difference in color and transparency of the pictures shows the liquid film structures are different from those for $H=0.5$ mm. When vapor quality is increasing, vapor slugs push and extend the liquid film and make it thinner. In the beginning, this film-extending effect works to improve heat transfer coefficient by increasing the film-covered surface area and at the same time decreasing thermal resistance of liquid film. With vapor generated more and more by enhanced evaporation, however, heat transfer begins to deteriorate at last as a result that the dry area is increased due to a rapid film consumption while the liquid replenishment is hindered by rapidly growing large vapor slug.

A smaller gap has no much space for isolated bubbles to freely grow without merging with other bubbles. When bubbles grow exceeding the gap size, they have to expand horizontally in the space and merge with other expanding bubbles. Consequently the region of bubbly flow, both of spherical bubbles and flattened bubbles, is restricted to a short flow length as the gap size is decreased, and the bubbly flow pattern is replaced with slug and annular flow more quickly in channels of smaller gaps. Thus the respective transition of flow patterns from (a) spherical bubbly, through (b) two-dimensional bubbly, (c) slug and bubbly and (d) slug, finally to (e) annular flow tends to occur at smaller vapor quality as the gap size is decreased.

An interesting finding obtained from the pictures in the slug flow regime, though not shown here, is that the heating surface under the vapor slug is covered by thin film, but a

filament form of liquid is also adhering on the surface. Some pictures both in the slug and annular flow regimes show the dark area covered by liquid film and the whitish area indicating dried surface. This confirms the coexistence of wetted area and dry area in these flow regimes. Disturbance waves are very rarely observed in the annular flow regime.

3.2 Heat Transfer

Local heat transfer coefficient, α, at five measurement locations of the heating wall temperature and heat flux (their distance from the inlet of the heated section is $z=10$, 30, 50, 70 and 90 mm, respectively) is defined as

$$\alpha=\frac{q}{T_w-T_f} \tag{1}$$

In Eq.(1), heat flux, q, and the heating wall temperature, T_w, are determined from the measured heating plate temperatures at respective locations by assuming one dimensional heat conduction. Fluid temperature, T_f, is calculated from an energy balance from the inlet to the point of interest. The energy balance gives fluid enthalpy at a distance of z from the inlet as

$$h=h_{in}+\frac{qz}{GH} \tag{2}$$

Here h_{in} is fluid enthalpy at the inlet, G mass velocity and H the gap size of channel. In the subcooled region where fluid enthalpy is less than the enthalpy of saturated liquid, $h\leq h_{sat}$, fluid temperature is calculated by assuming the specific heat of liquid c_{pL} is constant as

$$T_f=T_{in}+\frac{qz}{GHc_{pL}} \tag{3}$$

For the saturated region of $h\geq h_{sat}$, the saturation temperature is used as fluid temperature, T_f, in the defining equation (1) of heat transfer coefficient. In evaluating the saturation temperature and the saturation liquid enthalpy $h_{L,sat}$, fluid pressure is assumed as being linearly varied in the heated section and determined from the measured pressure drop across the test section. Equilibrium vapor quality, x, is calculated from an energy balance as follows and has negative or positive values depending on whether the fluid is subcooled or saturated.

$$x=-\frac{h_{L,sat}-h_{in}}{h_{fg}}+\frac{qz}{GHh_{fg}} \tag{4}$$

Here h_{fg} is the latent heat of evaporation. Heat flux in the above three equations is assumed piecewise uniform for the every heating section of 20 mm in the flow direction, the value of which is determined from the embedded thermocouples at the center of respective section. From Eq.(3) or (4), the subcooled inlet length is evaluated as

$$z_{sub}=\frac{GH(h_{L,sat}-h_{in})}{q}=\frac{GHc_{pL}(T_{sat}-T_{in})}{q} \tag{5}$$

Figure 5 shows a typical plot of data obtained in the experiment. The plotted data are the heating wall temperature T_w, the calculated fluid temperature T_f, the equilibrium vapor quality x, heat flux q, and heat transfer coefficient α. These data in **Fig. 5** are obtained for mass velocity of 100 kg/m^{2}s and the channel gap size of 0.5 mm. From these plots, it is clear that fluid temperature increases linearly along the flow direction up to the saturation point of $x=0$, thereafter decreases very slowly corresponding to a decrease in local fluid pressure

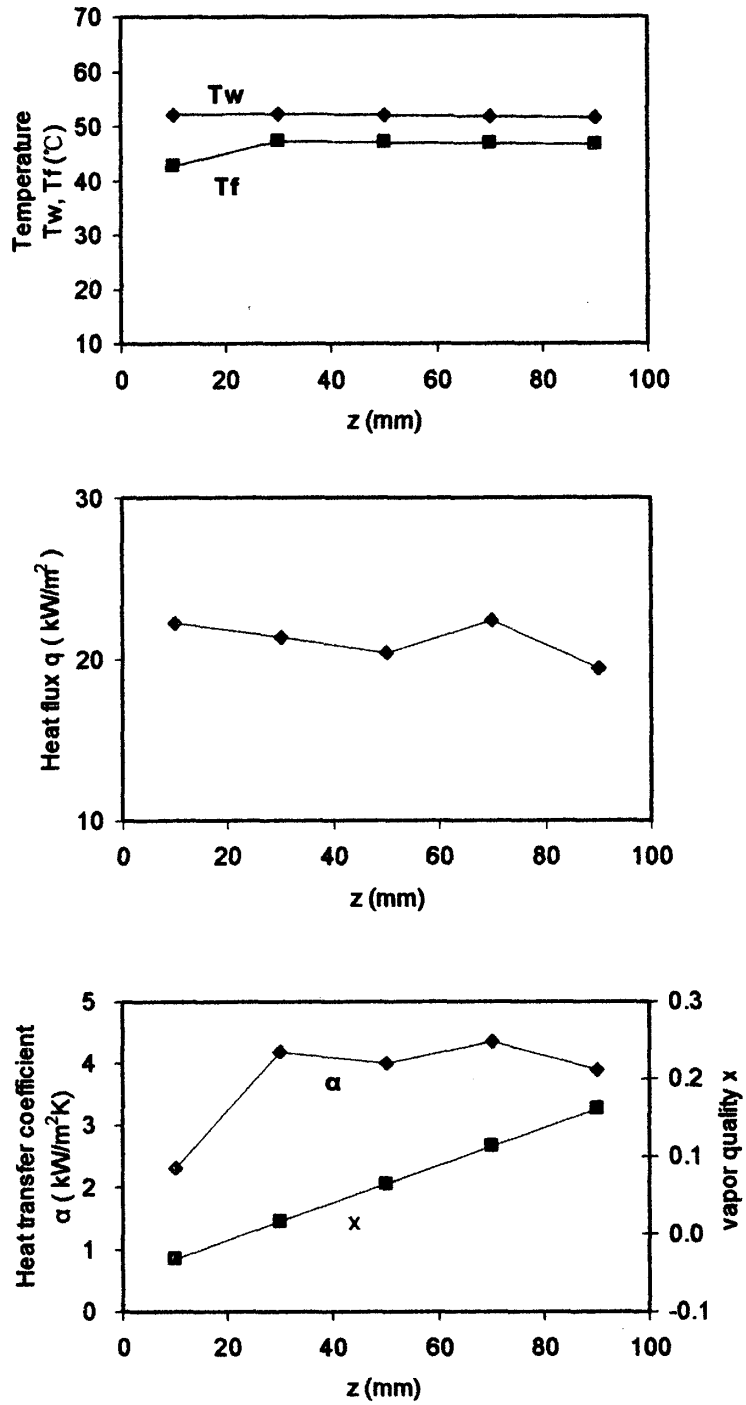

Fig. 5 Typical results for wall and fluid temperature, vapor quality, heat flux and heat transfer coefficient

due to the pressure drop in the test section. The wall temperature is to almost linearly increase up to an onset point of nucleation and then nonlinearly change in the flow direction. The maximum wall temperature is to appear downstream of the onset point of nucleation. In case of **Fig. 5** nucleation is considered to begin upstream of the first measurement location $z=50$ mm of the heating wall temperature. Heat fluxes at the five measurement locations show different values with a trend of the highest at $z=50$ mm and the lowest at $z=90$ mm. This trend is due to the end effect of the heating section. Heat transfer coefficient increases rapidly in the subcooled region as the saturation point is approached. In the saturated region, however, heat transfer coefficient is rather uniform or slowly decreasing in the flow direction

until vapor quality reaches some values. Thereafter heat transfer coefficient tends to increase in the flow direction.

3.3 Effect of Mass Velocity

Figure 6 shows heat flux transferred from the heating surface to fluid against the heating surface temperature, separately for the four different gap sizes of $H=0.2$, 0.5, 1.0 and 2.0 mm. For $H=0.5$, 1.0 and 2.0 mm, as the inlet fluid pressure was held nearly constant in measuring these data, the saturation temperature at the five measuring points of heat flux and surface temperature varies in a range 47 to 49°C. Because of a large pressure drop in the test section for a case of $H=0.2$ mm, the inlet pressure is especially higher, up to 0.13 MPa. Correspondingly the saturation temperature in this case is increased up to an amount 19°C.

Initial bubbles do not appear until the heating surface temperature exceeds the local

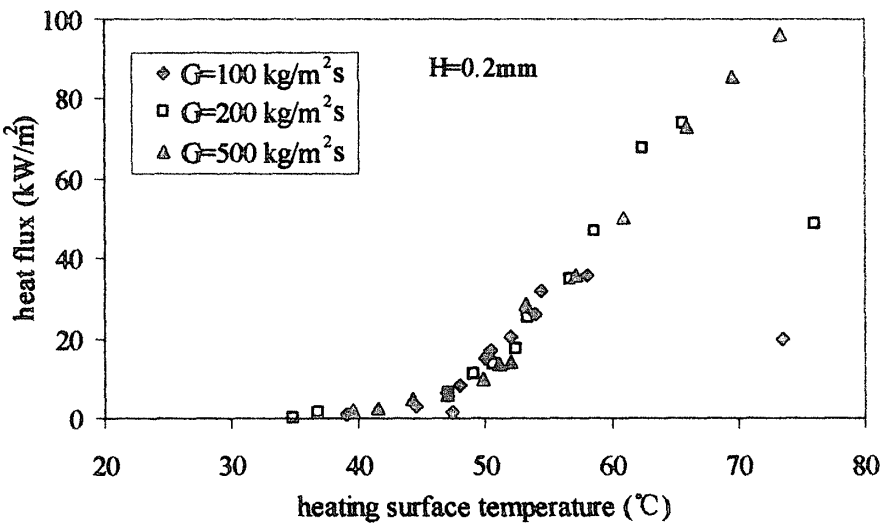

(a) H=0.2mm

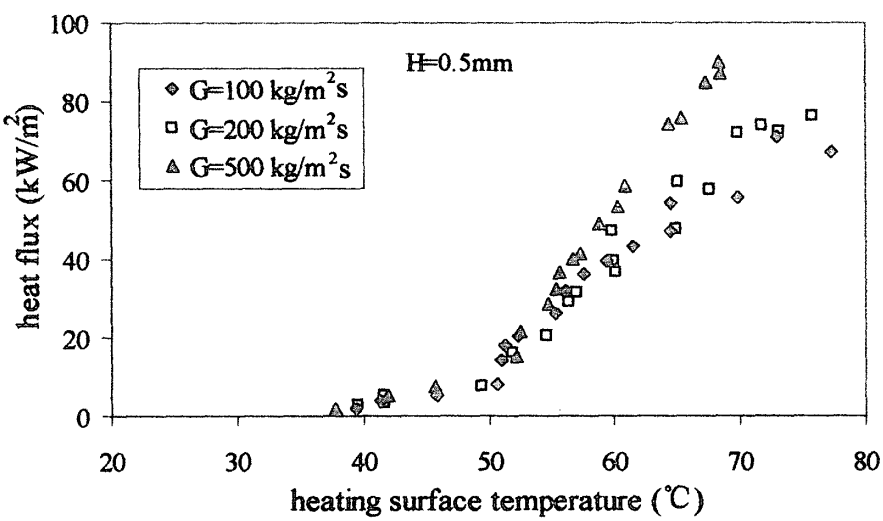

(b) H=0.5mm

Fig. 6 Heat flux against heating surface temperature

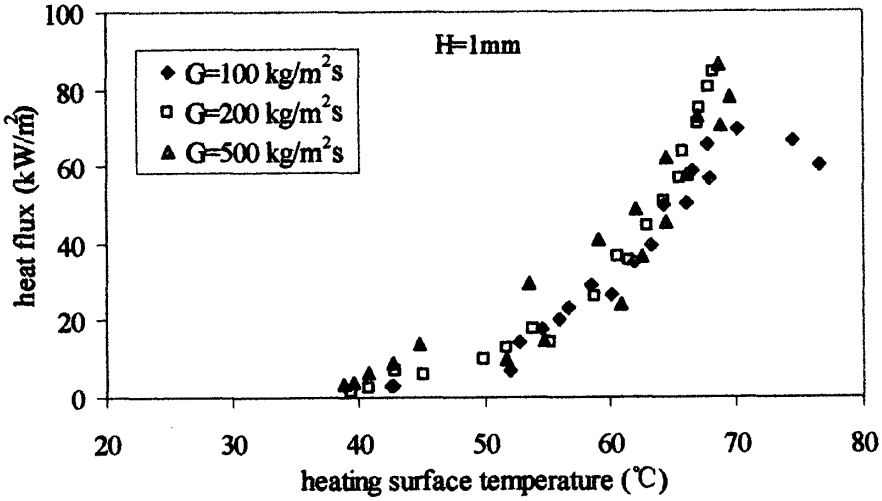

(c) H=1.0mm

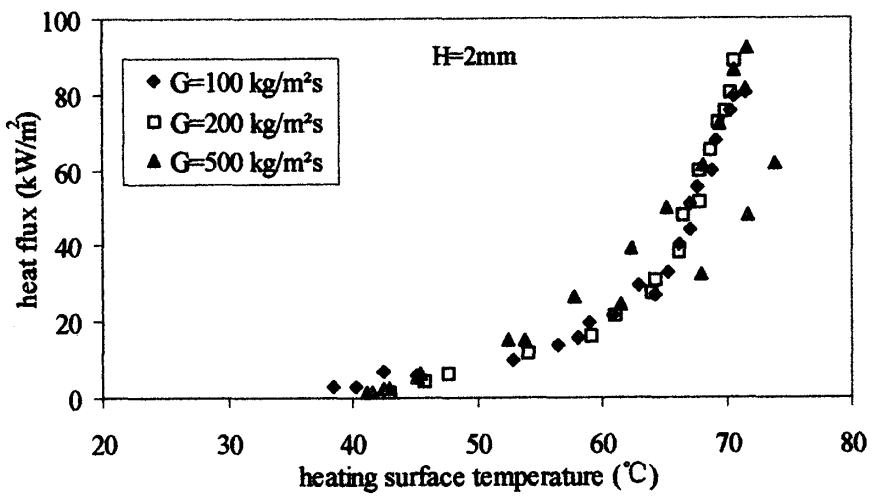

(d) H=2.0mm

Fig. 6 Heat flux against heating surface temperature

saturation temperature by a certain amount. Thereafter nucleate boiling is initiated, so that most data in **Fig. 6** are in the nucleate boiling region. It is evident from **Fig. 6** that the influence of mass velocity is insignificant at least on heat flux in the nucleate boiling region. A few data points deviating from the grouped data for $G=100$ kg/m^{2}s and $G=200$ kg/m^{2}s indicate heat transfer deterioration when the heating surface temperature is high and vapor quality is large.

From a comparison of the heat flux against wall temperature relationships in **Fig. 6**, heat flux transferred to fluid under the same heating wall temperature is found to increase as the gap size is decreased from $H=2.0$, to 1.0, 0.5, and 0.2 mm. Obviously from visual observation of boiling behavior, the heating surface temperature for nucleate boiling to onset is found to decrease as the gap size is decreased. Then heat flux increase rapidly from the onset point of nucleate boiling. Thus heat transfer coefficient is enhanced in the nucleate boiling region as the gap size of channel is reduced.

3.4 Effect of Gap Size

Figure 7 shows the same data as plotted in **Fig. 6** but rearranges them on the separate mass velocity of $G=100$, 200 and 500 kg/m^{2}s to indicate the effect of gap size. Clearly the

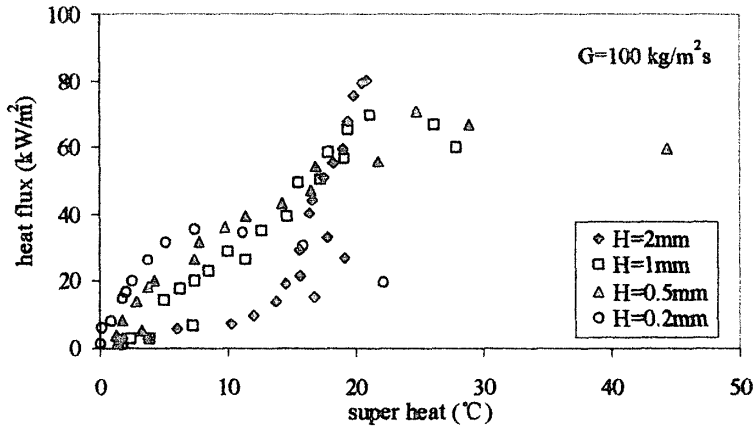

(a) G=100kg/m^{2}s

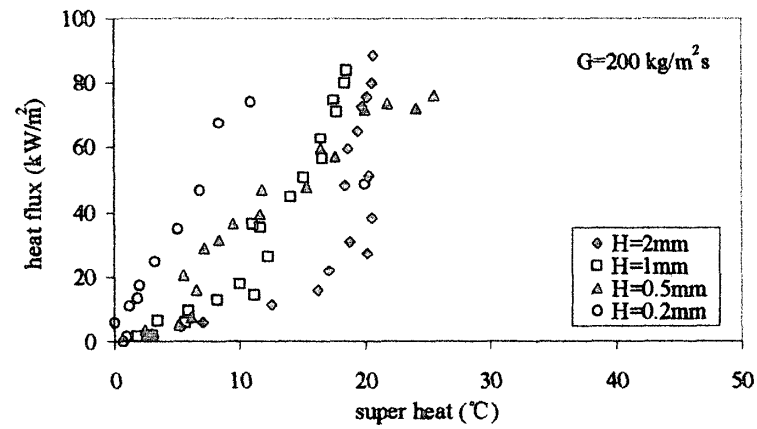

(b) G=200kg/m^{2}s

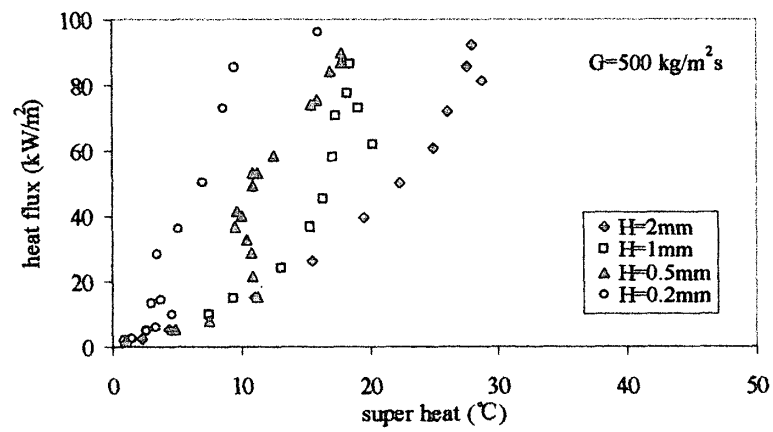

(c) G=500kg/m^{2}s

Fig. 7 Heat flux again superheat

smallest gap size of $H=0.2$ mm provides the highest heat flux irrespectively of mass velocity in so far as the heating surface temperature is considered as remaining in the nucleate boiling region. The difference of heat fluxes in this region for different gap sizes of channels becomes larger with increasing mass velocity. In every mass velocity, nucleate boiling onsets very early in the smallest gap of $H=0.2$ mm and thereafter heat flux increases very fast. As already clear from **Fig. 6**, mass velocity does not affect substantially heat transfer characteristics in the nucleate boiling region, whereas it certainly affects the critical heat flux. Influence of mass velocity on critical heat flux is most evident in **Fig. 7(a)** where the smallest gap size of $H=0.2$ mm has the lowest critical heat flux and the largest gap size of $H=2$ mm gives the highest value.

3.5 Effects of Heat Flux and Vapor Quality

Figure 8 shows heat transfer coefficient measured in the channel of a gap size of 0.5 mm as a function of vapor quality for two mass velocities of $G=100$ and 200 kg/m^{2}s. **Figure 8(a)** is for $G=100$ kg/m^{2}s and for two different heat fluxes of $q=20$ and 50 kW/m^2. **Figure 8(b)** is for heat flux of $q=50$ kW/m^2 and compares the data for two mass velocities of $G=100$ and 200 kg/m^{2}s. **Figure 8(c)** is for $G=200$ kg/m^{2}s and for three different heat fluxes of $q=20$, 50 and 90 kW/m^2. **Figure 8(d)** compares the data of $H=0.2$ and 0.5 mm at the same mass velocity of $G=100$ kg/m^{2}s and heat flux of $q=20$ kW/m^2. Plotted data are the local values at the central three locations of $z=30$, 50 and 70 mm, while the data at $z=10$ and 90 mm are deleted from these plots in consideration that those data may include the end effects and their accurate estimation is difficult. In these figures, it is evident that heat transfer coefficient is a very complex function of mass velocity, heat flux, and vapor quality for a given gap size of narrow channel.

As we can see in **Fig. 8(b)** the influence of mass velocity is insignificant in the saturated region of low quality up to around $x=0.2$. This fact suggests that convective heat transfer marginally contributes to the overall heat transfer in this low quality region and nucleate boiling is rather dominant there. In narrow channels of small gap sizes, spherical bubbles generated in nucleate boiling are rapidly deformed to two-dimensionally extended circular bubbles and merge each other so that the region of nucleate boiling is localized to a lower quality region compared to conventional size of channels. Especially in the present experiment the heating surface superheat is less than 5°C in the low quality region and this value is rather low compared to the heating surface superheat experienced in nucleate pool boiling of R-113 under the same saturation pressure[9]. Thus the nucleation ability is very weak and the number of nucleation sites is also very small in the present experiment. These factors are attributable to a very short length of the nucleate boiling dominance region.

At high vapor quality exceeding around 0.2, however, the influence of mass velocity becomes significant as seen in **Fig. 8(b)** with higher heat transfer coefficient at higher mass velocity. Flow regimes in such a high quality region are governed by slug flow to annular flow. Thus the convective evaporation from liquid film replaces with nucleate boiling, resulting in an occurrence of the influence of mass velocity to increase heat transfer coefficient at larger mass velocities.

As for the influence of vapor quality, the variation of heat transfer coefficient against vapor quality is very similar to that for channels of conventional under a certain condition, as exemplified in a case of $G=100$ kg/m^{2}s and $q=20$ kW/m^2 in **Fig. 8(a)**. With an increase of vapor quality, i.e., along the heating surface in the flow direction, heat transfer coefficient decreases at first in a low quality region and then begins to increase gradually for a further increase of quality and reaches a peak. Finally an abrupt decrease of heat transfer coeffi-

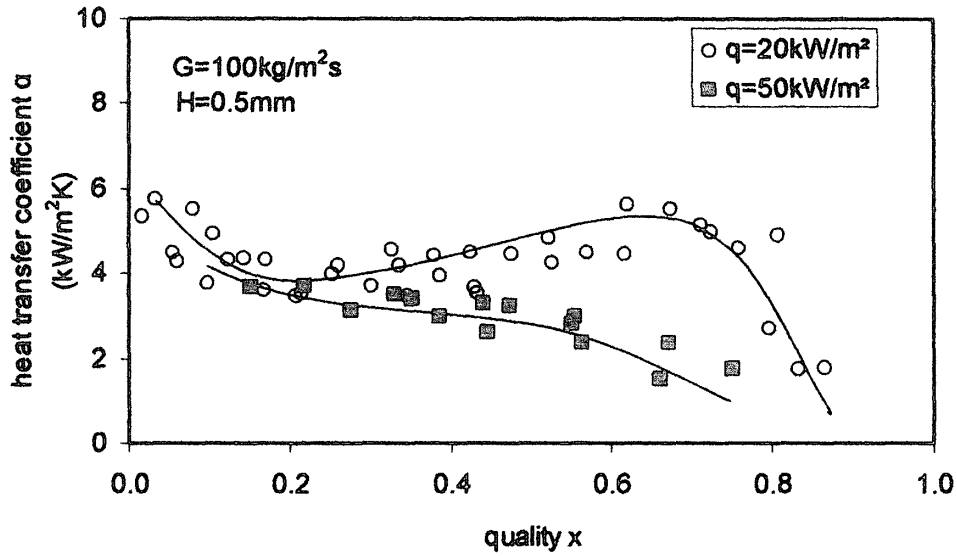

(a) G=100 kg/m²s, H=0.5mm

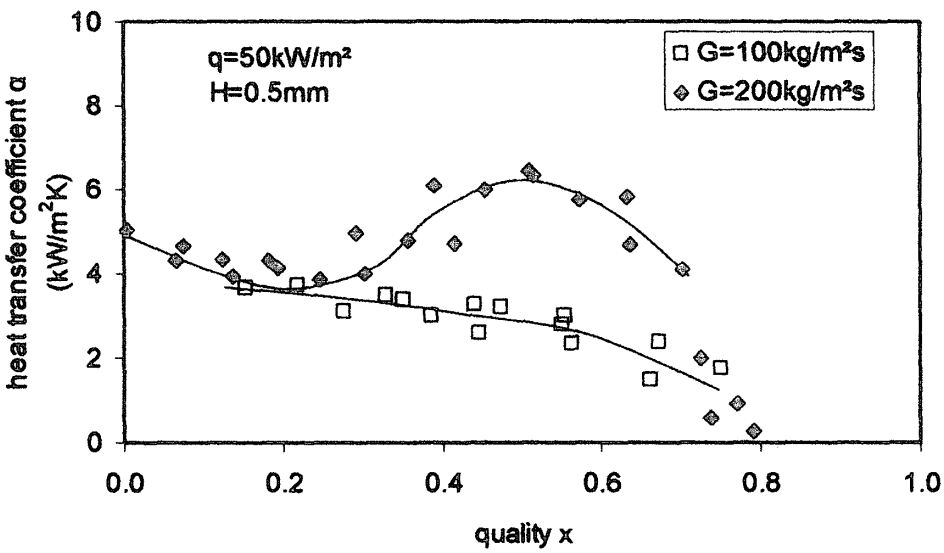

(b) q=500 kW/m², H=0.5mm

Fig. 8 Heat transfer coefficient against vapor quality

cient occurs at high vapor quality. Such a typical variation of heat transfer coefficient is correspondent to respective changes of heat transfer regimes from the onset of nucleate boiling, nucleate boiling dominance, convective evaporation dominance, dry-out and post dry-out heat transfer.

Two cases of $q=20$ and 50 kW/m^2 in **Fig. 8(c)** where mass velocity being doubled to 200 kg/m^{2}s indicate basically analogous variation of heat transfer coefficient as in the case of $G=100$ kg/m^{2}s and $q=20$ kW/m^2 shown in **Fig. 8(a)**.

For a case of $G=100$ kg/m^{2}s and $q=50$ kW/m^2 in **Fig. 8(a)**, heat transfer coefficient decreases almost over the whole quality region. A similar steady decrease of heat transfer coefficient is obtained for $G=200$ kg/m^{2}s, while at a higher heat flux of $q=90$ kW/m^2 as shown in **Fig. 8(c)**. This behavior of decreasing variation of heat transfer coefficient against

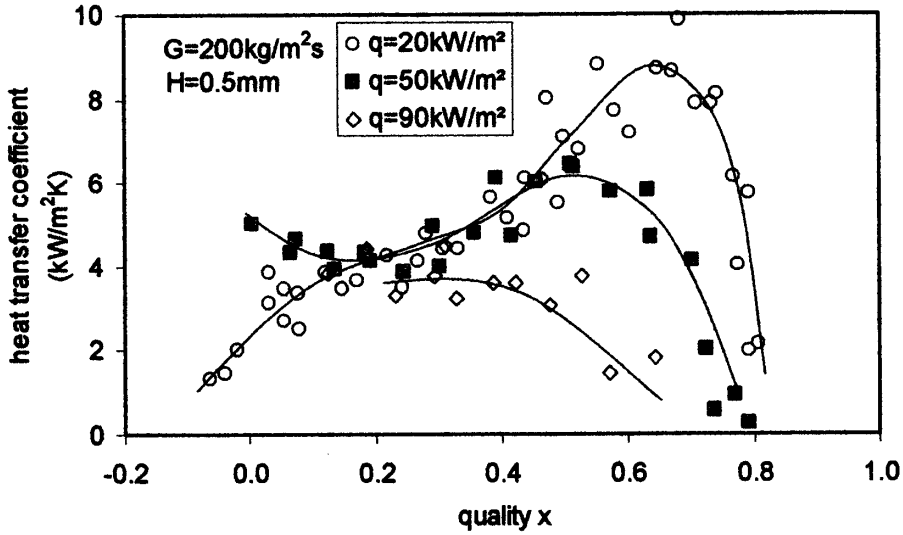

(c) G=200 kg/m²s, H=0.5mm

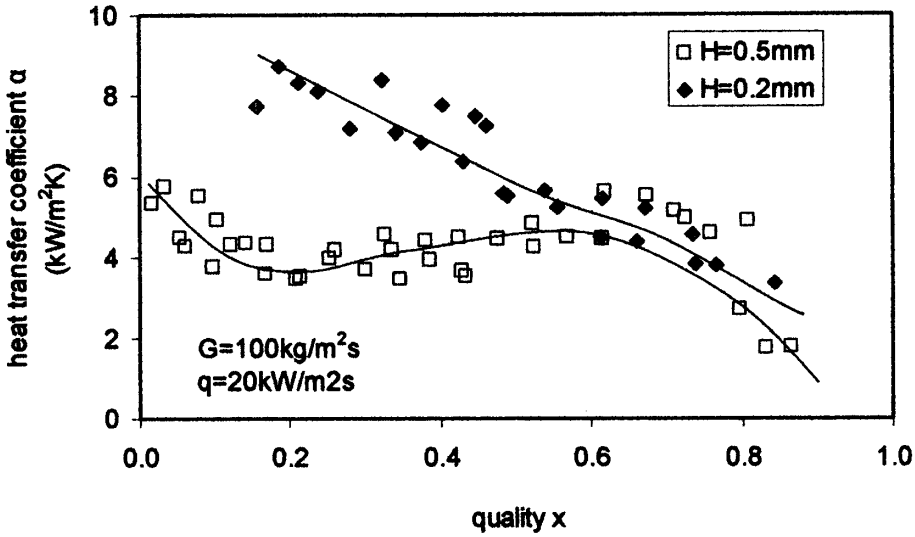

(d) G=100 kg/m²s, q=20kW/m²

Fig. 8 Heat transfer coefficient against vapor quality

vapor quality is very different from conventional results encountered in larger channels. It is not clear for now whether or not such a behavior is one of features characterizing boiling heat transfer in narrow channels. A plausible mechanism, if conjectured, may be deeply related to two-phase flow structure in narrow channels.

Figure 8(d) compares $H=0.2$ mm and $H=0.5$ mm at the same mass velocity $G=100$ kg/m²s and same heat flux $q=20$ kW/m². Once again we found $H=0.2$mm has better heat transfer coefficient in the lower quality region. Similarly to the cases of $q=50$ kW/m² in **Fig. 8(a)** and $q=90$ kW/m² in **Fig. 8(b)**, heat transfer coefficient of $H=0.2$ mm in **Fig. 8(d)** decreases very fast and superpose over the data of $H=0.5$ mm at the region of quality over 0.65.

According to visual examination of pictures recorded by the high-speed video camera, it is found that entrained droplets are not detected in slug and annular flow regimes. This is

a result of very rare occurrence of disturbance waves on annular film. Another finding from an examination of moving pictures is that a rather large size of dry patch steadily coexists on the heating surface with wetted area in an annular flow regime. In case of large size of channels, especially in round tubes, channel wall is considered as covered with liquid film, though thinning in the flow direction, and steadily wetted until the dry-out will occurs. Thus heat transfer coefficient continuously increases until a dry out quality is approached. In the present narrow channel of a small gap, however, slug and annular flows start after a short length of bubbly flow regime. Thus it is considered that the formation of dry patch will begin earlier when heat flux becomes higher and the area ratio of dry surface will increase in the flow direction until the surface is fully dried out. The coexistence of dry patch and wetted portion on the heating surface and a decrease of the effective wetted area with increasing vapor quality is likely attributable to the observed steady decrease of heat transfer coefficient in the flow direction. Further research is needed for validating this idea, so now under investigation.

4. Conclusion

Flow boiling heat transfer in narrow channels of rectangular cross section was studied experimentally and flow patterns were also observed. Finding in the present investigation is summarized as follows.

(1) Heat transfer coefficient is a complex function of mass velocity, heat flux and vapor quality for a given gap size of narrow channel.
(2) Small and micro-scale channel improves heat transfer characteristics in the low quality region. However, critical heat flux is deteriorated as the gap size is reduced.
(3) As observed in conventional size of channel, heat transfer is attributable to nucleate boiling in the low quality region where bubbly flow prevails, and in the succeeding slug and annular flow regions convective evaporation from thin liquid film contributes to heat transfer.
(4) For high boiling number, i.e., when heat flux is high relative to mass velocity, heat transfer coefficient decreases in the flow direction in slug and annular flow regions. This behavior considered as relevant features to narrow channels may be caused by coexistence of dry patch and wetted area portion on the heating surface beneath vapor slugs. Decreasing wetted surface area in the flow direction is likely an influential factor on heat transfer in this region of narrow channels.
(5) Five flow patterns are identified: bubbly flow of spherical bubbles, bubbly flow of two-dimensionally flattened bubbles, slug and bubbly flow, slug flow, and annular flow.
(6) Flow pattern transition to the slug and annular flow occurs at lower quality as the gap size is decreased. Thus the length of bubbly flow, i.e., the region of nucleate boiling dominance is shortened down to vapor quality less than 0.2 at most.

Nomenclature

c_{pL} : specific heat of liquid, J/kgK
G : mass velocity, kg/m^{2}s
h : enthalpy, J/kg
h_{in} : inlet fluid enthalpy, J/kg
h_{fg} : latent heat of evaporation, J/kg
$h_{L,sat}$: enthalpy of saturated liquid, J/kg

H : gap of channel, m or mm
q : heat flux, W/m^2 or kW/m^2
T_f : mean fluid temperature, K or °C
T_{in} : inlet fluid temperature, K or °C
T_{sat} : saturation temperature, K or °C
T_w : wall temperature, K or °C
x : vapor quality, dimensionless
z : flow length from the inlet of the heated section, m or mm
α : heat transfer coefficient, W/m^2K or kW/m^2K

References

1) Peng, X. F., Wang, B. X., Peterson, G. P., and Ma, H. B., Experimental Investigation of Heat Transfer in Flat Plates with Rectangular Microchannels, Int. J. Heat Mass Transfer, Vol.38(1995), pp.127-137.
2) Bao, Z. Y., Fletcher, D. F., and Haynes, B. S., Flow Boiling Heat Transfer of Freon R11 and HCFC123 in Narrow Passages, Int. J. Heat Mass Transfer, Vol.43(2000), pp.3347-3358.
3) Lin, S., Kew, P. A., and Cornwell, K., Two-Phase Heat Transfer to a Refrigerant in a 1 mm Diameter Tube, Int. J. Refrigeration, Vol.24(2001), pp.51-56.
4) Fujita, Y., Ohta, H., Uchida, S., and Nishikawa, K, Nucleate Boiling Heat Transfer and Critical Heat Flux in Narrow Space between Rectangular Surfaces, Int. J. Heat Mass Transfer, Vol.31(1988), pp.229-239.
5) Yu, W., France, D. M., Wambsganss, M. W., and Hull, J. R., Two-Phase Pressure Drop, Boiling Heat Transfer, and Critical Heat Flux to Water in a Small-Diameter Horizontal Tube, Int. J. Multiphase Flow, Vol.28(2002), pp.927-941.
6) Tran, T. N., Wambsganss, M. W., and France, D. M., Small Circular- and Rectangular-Channel Boiling with Two Refrigerants, Int. J. Multiphase Flow, Vol.22 (1996), pp.485-498.
7) Triplett, K. A., Ghiaasiaan, S. M., Abdel-Khalik, S. I.,. and Sadowski, D. L., Gas-Liquid Two-Phase Flow in Microchannels Part I: Two-Phase Flow Patterns, Int. J. Multiphase Flow, Vol.25(1999), pp.377-397.
8) Xu, J., Experimental Study on Gas-Liquid Two-Phase Flow Regimes in Rectangular Channels with Mini Gaps, Int. J. Heat Fluid Flow, Vol.20(1999), pp.422-428.
9) Nishikawa, K., Fujita, Y., Ohta, H., and Hidaka, S., Heat Transfer in Nucleate Boiling of Freon, Heat Transfer-Japanese Research, Vol.8 (1979), pp.16-36.